Sensitization Effect of Porphyrin Dye on the Photocurrent of Al/Polythiophene Schottky-Barrier Cells

Kohshin Takahashi,*,† Madoka Asano,† Kiyoaki Imoto,‡ Takahiro Yamaguchi,† and Teruhisa Komura†

Department of Chemistry and Chemical Engineering, Faculty of Engineering, Kanazawa University, Kodatsuno, Kanazawa 920-8667, Japan, and Division of Applied Science, Graduate School of Natural Science and Technology, Kanazawa University, Kodatsuno, Kanazawa 920-8667, Japan

Jyun-ichi Nakamura‡,§ and Kazuhiko Murata*,||

Performance Chemicals and Materials Research Center, Nippon Shokubai Co., Ltd., 5-8, Nishi Otabi-cho, Suita, Osaka, 564-8512, Japan, and New Business Planning, Nippon Shokubai Co., Ltd., Koraibashi, Osaka 564-0041, Japan

Received: September 5, 2002; In Final Form: December 10, 2002

An enhanced photocurrent was obtained in an Al/porphyrin-sensitized regioregular polythiophene (PTh) Schottky-barrier cell when the top energy level of the valence band of PTh solid was more negative than the HOMO energy level of porphyrin. However, when ortho-substituted *meso*-phenylporphyrins were employed, the photocurrent enhancement decreased to about half compared to the case when nonsubstituted *meso*-phenylporphyrins were used. We conclude from these results that both a larger thermodynamic driving force for a photoinduced hole transfer from porphyrin to PTh and a closer distance between the two conjugating planes of porphyrin and PTh are necessary to obtain a larger photocurrent.

Introduction

It has been a long time since organic solar cells were expected as the candidate for a low cost solar cell. However, practical use of them has not been attained because the electrical resistance and the charge-carrier mobility of the organic dyes typically used in such cells were limited compared to inorganic semiconductors. To overcome the problem of lower mobility for organic semiconductors, using soluble conjugated polymer as the charge-transport material seems to be successful.[1−16] Sariciftci et al. demonstrated that the cell consisting of fullerene/PPV shows an energy conversion yield of 3% under AM1.5 illumination.[9,10] On the other hand, we have reported in a series of papers that mixing two types of dye in the organic solar cells significantly improved the photovoltaic property compared to the case of using the dyes solely.[17−21] The reason for photocurrent enhancement in the mixed dyes cells is that photoinduced intermolecular charge transfer from one dye to the other propels effective charge separation.

Because we supposed combining the above two ways promises further improvement, we prepared organic solar cells consisting of the mixture of a conjugated polymer as the better charge-transport material and a dye as the more effective light-harvesting material. We recently reported preliminarily that the enhanced photocurrent was observed for the organic solar cells with a mixture of regioregular polythiophene (PTh) and a dye such as a porphyrin or a merocyanine.[14−16] However, little is known about the mechanism of photocurrent enhancement in the cell with a conjugated polymer and a dye because the number of studies for the system is restricted, which are done by Sicot et al.[11−13] and by us.[14−16]

In this paper, we will clarify the mechanism of photocurrent enhancement in the Al/PTh+porphyrin Schottky-barrier solar cell. Various porphyrins with different substituents were employed in the cell to examine which of the following possible factors are dominant for the photocurrent enhancement. We checked the effect of (1) a built-in electric field in the cell, (2) the specific resistivity of the mixture, (3) photoinduced charge transfer between PTh and porphyrin, and (4) space distance between porphyrin and PTh.

Experimental Section

Tetraphenylporphyrin derivatives as shown in Figure 1 were synthesized and purified as literature methods.[22,23] A regioregular polythiophene, PTh (poly(3-hexylthiophene-2,5-diyl), average molecular weight is ca. 87 000), was purchased from Aldrich Chemicals and used without further purification.

Sandwich-type photocells of Al/porphyrin+PTh/Au were fabricated as in previous papers.[19,21] A mixed chloroform solution of the porphyrin dye and polythiophene was dropped onto a vacuum-deposited Al film on a slide glass making the spin-coated film. The photoactive area was confined to 0.25 cm^2. The molar mixing ratio R of porphyrin to thiophene unit in PTh and the thickness d of the spin-coated films were estimated from the amount and the density of porphyrin and PTh on the substrate. The same density of 1.3 g cm^{-3} was assumed for both compounds.

The measurements of the photocurrent action spectra, the current−voltage curves, and the specific resistivity of organic solid films were made as in previous papers.[19,21] The prepared

† Department of Chemistry and Chemical Engineering, Kanazawa University.
‡ Division of Applied Science, Kanazawa University.
§ Performance Chemicals and Materials Research Center, Nippon Shokubai Co. Ltd.
|| New Business Planning, Nippon Shokubai Co., Ltd.

10.1021/jp022001e CCC: $25.00
Published on Web 01/21/2003

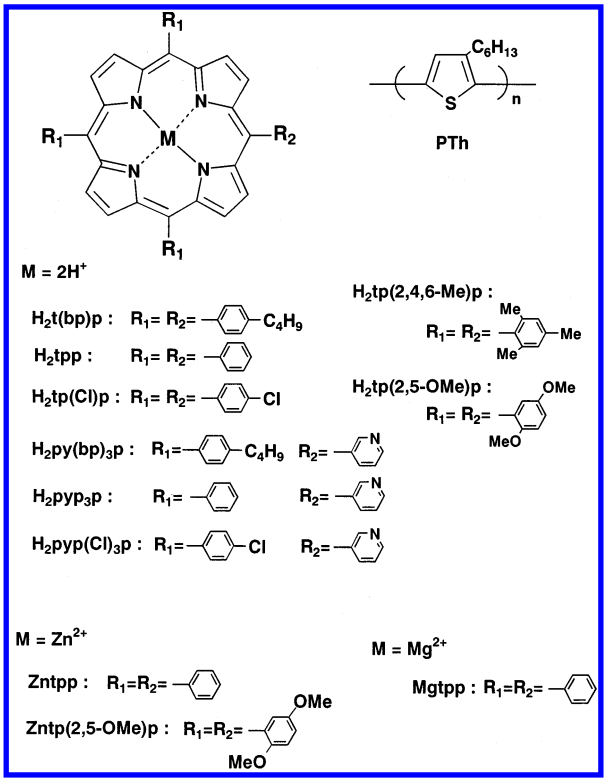

Figure 1. Structures and abbreviations of regioregular polythiophene and porphyrins.

cell was kept in a dark sealed vessel that contained silica gel as the drying agent for 1 day at room temperature to protect the Al electrode from photocorrosion obtaining a steady photocurrent.[24,25] All electrical measurements were performed in the drying vessel equipped with optical windows at room temperature. The measurement of capacitance−voltage characteristics was carried out with a low-frequency oscillographic method under computer control.[26,27] The ramp potential with a frequency of 0.03−0.04 Hz generated by an Advantest TR8652 electrometer was applied to the Al/porphyrin+PTh/Au sandwich-type cell, and the dark current was measured simultaneously by this electrometer.

Cyclic voltammetry was also performed as in previous papers.[19,21] The electrode potential was described on the basis of the half-wave potential of ferrocenium ion/ferrocene (Fc^+/Fc). The absorption spectra of solid films formed on a slide glass were recorded on a Hitachi U-3210 UV−visible spectrometer.

Results and Discussion

Figure 2 shows short-circuit photocurrent action spectra of the cells with pure PTh, pure porphyrins, and porphyrin+PTh mixed solids, accompanying their absorption spectra on the glass substrate. The mixing ratio R was defined as the molar ratio of porphyrin to thiophene unit in PTh. For all Schottky-barrier solar cells tested in this work, the action spectra for Al side irradiation roughly followed the absorption spectra, and a smaller photocurrent for Au side irradiation, so-called optical filter effect of the photocurrent was observed. That is, the Schottky barrier was formed at the interface between low work function Al and the mixed solid with a p-type conductance, and the excited porphyrins and/or the excited PTh contributed to the photocurrent generation. The location of the Schottky barrier can also be confirmed by the shift of the maxima of current during

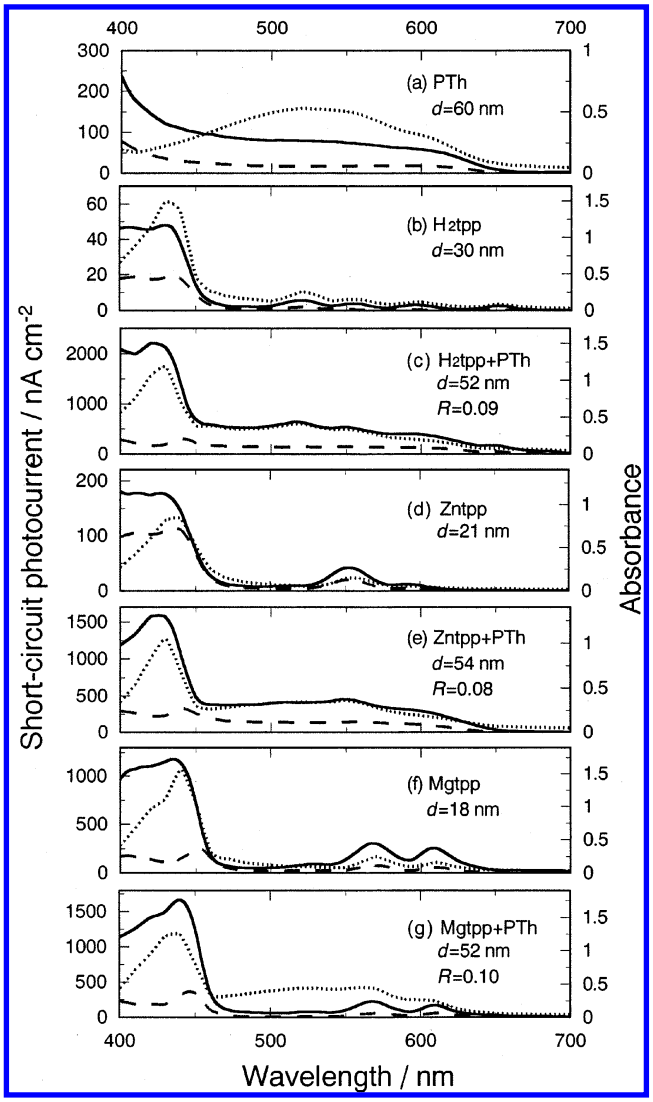

Figure 2. Photocurrent action spectra of Al/organic solid Schottky-barrier cells (Al side irradiation (—), Au side irradiation (- - -)) and absorption spectra on a glass substrate (•••). R and d indicate the mixing molar ratio and film thickness, respectively. The light intensity at the metal/organic solid interface was normalized to 50 μW cm^{-2}.

illumination through the Au electrode, shown by the broken lines in Figure 2.

An enhanced photocurrent was observed for the mixed cells of H_2tpp+PTh and Zntpp+PTh compared to the cells of the pure porphyrins or the pure PTh. To illustrate clearly such a remarkable increment of the photocurrent, the dependence of short-circuit photocurrent quantum yield ϕ at the Soret peak of porphyrin on film thickness d was shown for the pure H_2tpp cell and the H_2tpp+PTh mixed cell, as shown in Figure 3. The ϕ value is calculated by the following equation,

$$\phi\,(\%) = 124 J_{sc}/(I_0 \lambda) \qquad (1)$$

where J_{sc} is the short-circuit photocurrent in units of nA cm^{-2}, I_0 (μW cm^{-2}) is the light intensity at metal/organic solid interface, and λ (nm) is the incident light wavelength. On the other hand, returning to Figure 2, the photocurrent for the pure Mgtpp cell was as large as that for the Mgtpp+PTh mixed cell. This reason is clarified later. It was found from careful observation that the action spectra of H_2tpp+PTh and Zntpp+PTh cells for Al side irradiation considerably fitted with the absorption spectra, but the action spectrum of the Mgtpp+PTh

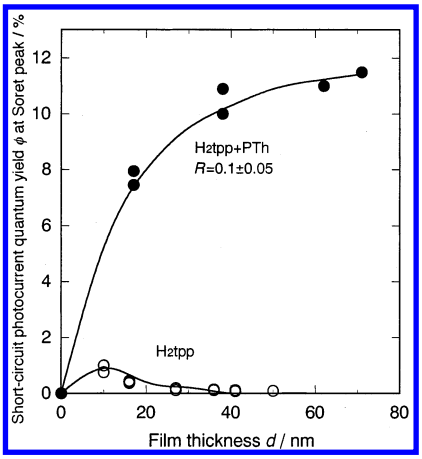

Figure 3. Film thickness d dependence of short-circuit photocurrent quantum yield ϕ at Soret peak of porphyrin for Al side irradiation in pure H_2tpp and mixed H_2tpp+PTh ($R = 0.1 \pm 0.05$) photocells.

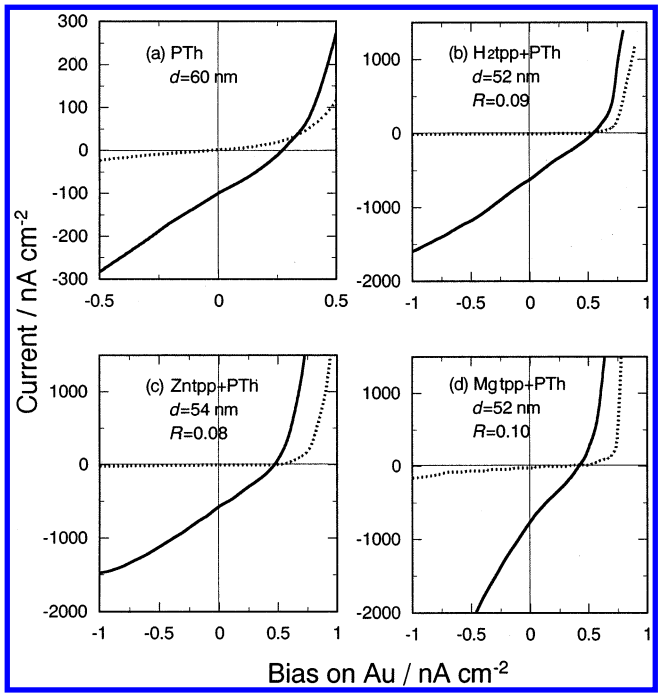

Figure 4. Current−voltage characteristics of Al/organic solid Schottky-barrier cells in the dark (···) and under illumination (—). A 550 nm monochromatic light for pure PTh cell (a), and a 435 nm monochromatic light for mixed cells (b), (c), and (d) were irradiated from Al side. The light intensity at the Al/organic solid interface was 53 μW cm^{-2} for the pure PTh cell (a), 16 μW cm^{-2} for the H_2tpp+PTh cell (b) and the Zntpp-PTh cell (c), and 20 μW cm^{-2} for the Mgtpp-PTh cell (d).

cell did not follow the absorption spectra above 500 nm of wavelength where the PTh film has the absorption. The reason that the photocurrent profile is classified into two categories will be discussed later.

Figure 4 shows current−voltage $J-V$ curves of pure PTh (a), H_2tpp+PTh (b), Zntpp+PTh (c), and Mgtpp+PTh (d) cells. The dark $J-V$ curves exhibiting better rectification property, and unsaturated photocurrents by space-charge limitation were obtained by applying negative bias on the Au electrode. The photovoltaic properties of short-circuit photocurrent quantum yield ϕ, open-circuit photovoltage V_{oc}, fill factor ff, and energy conversion yield η for Al side irradiation at a maximal absorption peak wavelength λ under an optimum condition were summarized in Table 1. The ff and η values are calculated by

TABLE 1: Performance of Al/Organic Solid/Au Sandwich-Type Photocells for Al Side Irradiation of Monomeric Light λ under Optimum Condition[a]

organic solid	λ (nm)	R[b]	d (nm)[c]	ϕ (%)[d]	V_{oc} (V)[e]	ff[f]	η (%)[g]
PTh	550		60	0.34	0.27	0.29	0.012
H2tpp	435		24	0.60	0.35	0.23	0.017
H2tpp+PTh	430	0.04	51	11.2	0.59	0.27	0.62
Zntpp	435		21	0.87	0.55	0.22	0.037
Zntpp+PTh	435	0.08	54	10.1	0.47	0.28	0.47
Mgtpp	440		18	7.6	0.51	0.25	0.34
Mgtpp+PTh	435	0.10	52	10.5	0.54	0.24	0.48

[a] The light intensity was about 20 μW cm^{-2} at the Al/organic solid interface. [b] Molar ratio of porphyrin to thiophene unit in PTh. [c] Film thickness. [d] Short-circuit photocurrent quantum yield. [e] Open-circuit photovoltage. [f] Fill factor. [g] Energy conversion yield.

the following equations,

$$ff = J_{max}V_{max}/(J_{sc}V_{oc}) \quad (2)$$

$$\eta\ (\%) = J_{sc}V_{oc}ff/(10I_0) \quad (3)$$

where $J_{max}V_{max}$ is the maximum power output of the cell in unit of nW cm^{-2}, $J_{sc}V_{oc}$ (nW cm^{-2}) is the ideal power output, and I_0 (μW cm^{-2}) is the light intensity at the metal/organic solid interface. Among the pure porphyrin cells tested, the largest short-circuit photocurrent quantum yield ϕ was obtained for the Mgtpp cell. This is because Mgtpp is oxidized more easily; the physisorbed oxygen molecules to Mgtpp solid become a more efficient dopant,[28] and after all, the electrical resistivity of the solid is the lowest one. In fact, the specific resistivity r varied in the order Mgtpp < Zntpp ≪ H_2tpp as the oxidation became easier in the order of Mgtpp > Zntpp > H_2tpp; see the r values in Table 2 and the arrows (oxidation potentials) in Figure 6. The ϕ values of the mixed solid cells of H_2tpp+PTh and Zntpp+PTh were larger than those of the corresponding pure porphyrin and PTh cells. The mixed solid cells H_2tpp+PTh and Zntpp+PTh consequently showed larger energy conversion yields η compared to the corresponding pure porphyrin and PTh cells.

Effect of Built-in Electric Field in the Cell. The capacitance of the Schottky barrier at the Al/PTh and Al/porphyrin+PTh interfaces was measured in the dark as a function of the applied voltage by a low-frequency oscillographic method using a triangle wave.[26,27] When the applied ramp bias increases, the observed current J_+ is a sum of charging and ohmic currents,

$$J_+ = C(\mathrm{d}V/\mathrm{d}t) + V/rr \quad (4)$$

where C is the capacitance, V is the applied voltage, dV/dt is the scan rate of the applied voltage, and rr is the resistance. When the voltage decreases, the current J_- is a sum of discharging and ohmic currents,

$$J_- = -C(\mathrm{d}V/\mathrm{d}t) + V/rr \quad (5)$$

Combining above two equations, the capacitance is obtained as

$$C = (J_+ - J_-)/2(\mathrm{d}V/\mathrm{d}t) \quad (6)$$

Further, because dV/dt is given by $4V_0f$, where V_0 is the amplitude of the applied voltage and f is the frequency of the ramp bias, the following equation is obtained,

$$C = (J_+ - J_-)/8V_0f \quad (7)$$

TABLE 2: Density of Ionized Carriers in the Solid (N), Width of Depletion Layer under Short-Circuit Condition (W_{sc}), and Built-in Potential (V_b) Estimated by Measuring Electric Capacitance of Al/Organic Solid Schottky-Barrier Cells and Specific Resistivity (r)

organic solid	N (10^{17} cm^{-3})	W_{sc} (nm)	V_b (V)	V_b/W_{sc} (10^5 Vcm^{-1})	r (Ω cm)
PTh	6 ± 2	22 ± 3	0.6 ± 0.1	2.7	2×10^5
H2tpp				0.8[a]	ca. 10^{14} [a]
H2tpp+PTh ($R = 0.09$)	10 ± 10	13 ± 2	0.5 ± 0.1	3.8	3×10^5
Zntpp	0.6[b]	90[b]	1[b]	1.1,[b] 2.9[c]	3×10^{10} [c]
Zntpp+PTh ($R = 0.10$)	8 ± 2	15 ± 2	0.5 ± 0.1	3.3	
Mgtpp	30 ± 20	6 ± 4	0.9 ± 0.2	15	1×10^9
Mgtpp+PTh ($R = 0.10$)	50 ± 10	7 ± 1	0.7 ± 0.1	10	

[a] Cited from ref 25. The solid film is made by spin-coating. [b] Cited from ref 29. The solid film is made by vacuum-deposition. [c] Cited from ref 19. The solid film is made by spin-coating.

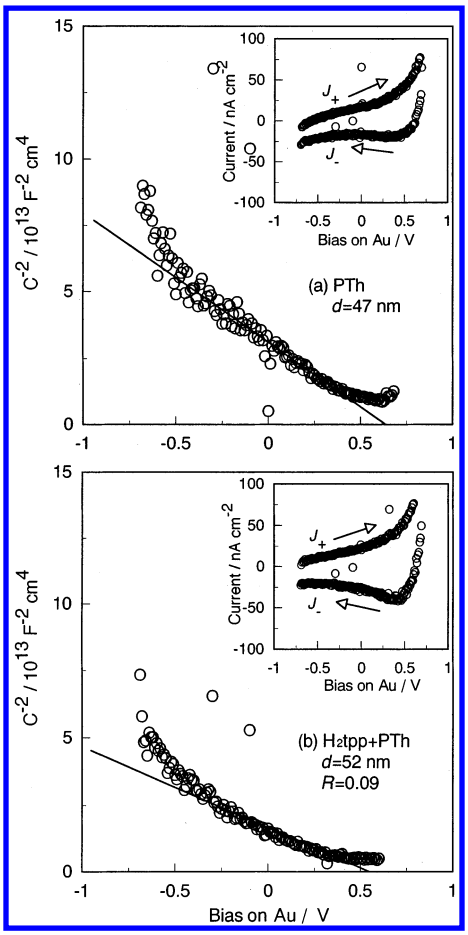

Figure 5. Mott−Schottky plots for Al/PTh ($d = 47$ nm) (a) and Al/H_2tpp + PTh ($R = 0.09$, $d = 52$ nm) (b) Schottky-barrier cells. Insets show dark current−voltage curves at 0.033 Hz for the PTh cell (a) and at 0.035 Hz for the H_2tpp+PTh cell (b). The arrows in the insets show the direction of the potential sweep. See text for the definition of J_+ and J_- in the insets.

When the current density is used for J_+ and the J_-, C represents the capacitance per unit area. The inset in Figure 5a shows the current−voltage curve under application of a ramp bias between −0.7 and +0.7 V ($V_0 = 0.7$ V) at $f = 0.033$ Hz. When the Poisson equation is solved, the width of the depletion layer W is expressed as a function of the bias,

$$W = [2\epsilon\epsilon_0(V_b - V)/eN]^{1/2} = \epsilon\epsilon_0/C \qquad (8)$$

where N is the density of the ionized carriers in the solid, e is the electron charge, ϵ is the relative dielectric constant, ϵ_0 is the vacuum permittivity, and V_b is the built-in potential of the Schottky barrier. By rearranging the above equation, we can

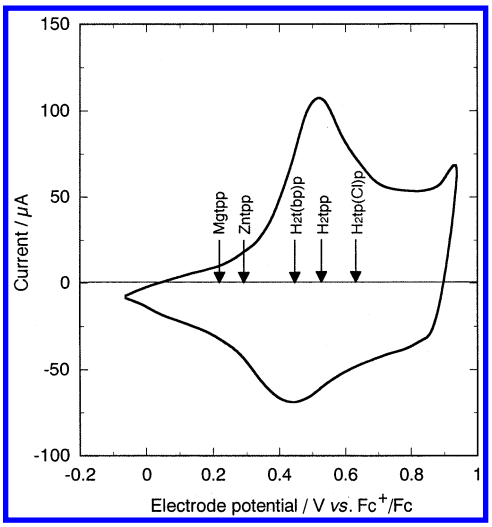

Figure 6. Cyclic voltammogram of PTh film electrode in acetonitrile solution containing 0.1 mol dm^{-3} tetraethylammonium perchlorate. The scan speed was 10 mV s^{-1}. The active area of the PTh film electrode was 0.25 cm^2. The arrows show the oxidation potential of porphyrins in dichloromethane.

obtain the following relation,

$$C^{-2} = 2(V_b - V)/\epsilon\epsilon_0 eN \qquad (9)$$

As shown in Figure 5a, the plot of C^{-2} against V (Mott−Schottky plot) for the Al/PTh Schottky-barrier cell gave a straight line in the range between −0.5 and +0.4 V. We obtained the values of $V_b = 0.6 \pm 0.1$ V, $N = (6 \pm 2) \times 10^{17}$ cm^{-3}, and $W_{sc} = 22 \pm 3$ nm assuming $\epsilon = 4$, where W_{sc} is the width of the depletion layer under a short-circuit condition. Further, by the Mott−Schottky plot for the Al/H_2tpp+PTh ($R = 0.09$) Schottky-barrier cell shown in Figure 5b, we obtained the values of $V_b = 0.5 \pm 0.1$ V, $N = (1 \pm 1) \times 10^{18}$ cm^{-3}, and $W_{sc} = 13 \pm 2$ nm. The N value of the mixed solid was larger compared to that of the pure PTh solid because of an electronic interaction between H_2tpp and PTh. After all, the W_{sc} value of the mixed cell was smaller than that of the pure PTh cell. The results for the Al/Zntpp+PTh ($R = 0.10$), Al/Mgtpp, and Al/Mgtpp+PTh ($R = 0.10$) Schottky-barrier cells are summarized in Table 2. Further, these values for the Al/H_2tpp and Al/Zntpp Schottky-barrier cells are cited from refs 19, 25, and 29, being summarized in Table 2.

Because the photoproduced electrons and holes at the Al/organic solid interface are separated by the electric field formed in the Schottky barrier and eventually the photocurrent is observed due to the charge-separation, the estimation of the electric field is important. We estimated from the values of V_b and W_{sc} that the potential gradient V_b/W_{sc} under short-circuit condition in the Schottky barrier was 3×10^5 V cm^{-1} for the

pure PTh cell, 0.8×10^5 V cm^{-1} for the pure H_2tpp cell, and 4×10^5 V cm^{-1} for the H_2tpp+PTh cell. The V_b/W_{sc} values are summarized in Table 2. The order of the electric field, H_2tpp+PTh ≈ PTh > H_2tpp, did not agree with that of the short-circuit photocurrent quantum yield ϕ, H_2tpp+PTh ≫ PTh > H_2tpp. Further, the order of the electric field, Zntpp+PTh ≈ PTh ≈ Zntpp, did not agree with that of the short-circuit photocurrent quantum yield ϕ, Zntpp+PTh ≫ Zntpp > PTh. Therefore, this factor is not the most relevant factor for enhancing the photocurrent of the H_2tpp+PTh and Zntpp+PTh cells.

Effect of the Specific Resistivity. The specific resistivity r of solid films is generally important for determining the photocell performance. The r value was ca. 10^{14} Ω cm for the pure H_2tpp solid,[25] 2×10^5 Ω cm for the pure PTh solid, and 3×10^5 Ω cm for the H_2tpp+PTh mixed solid ($R = 0.09$). The relatively small resistivity of the pure PTh solid and the H_2tpp+PTh mixed solid is ascribed to the relatively large hole mobility in regioregular polythiophene solids (ca. 10^{-3} to 10^{-4} cm^2 V^{-1} s^{-1}) as reported previously,[30,31] where regioregularity and conjugation coenhance the mobility. On the other hand, the hole mobility of the pure porphyrin solid was very small, namely, ca. 10^{-16} cm^2 V^{-1} s^{-1} for the H_2tpp solid[32] and ca. 10^{-10} cm^2 V^{-1} s^{-1} for the Zntpp solid.[33] Because the resistivity of the H_2tpp+PTh or Zntpp+PTh mixed solid could be much smaller than that of the pure H_2tpp or Zntpp solid, the photocell performance was much better for the mixed cell than for the pure H_2tpp or Zntpp cell. However, the difference of the performance of the pure PTh cell and the mixed cells cannot be explained by this factor, because both the resistivities of the pure PTh solid and the mixed solids were almost the same.

Effect of Photoinduced Hole Transfer from Porphyrin to PTh. We previously reported that the photocurrent of the Schottky-barrier cell with a porphyrin heterodimer solid was remarkably enhanced because of a photoinduced electron transfer from zinc porphyrin to metal-free porphyrin in the porphyrin heterodimer.[17,21] Therefore, whether a photoinduced charge transfer can occur between porphyrin and PTh was examined by estimating their energy levels. The cyclic voltammogram for the oxidation (that is, p-type doping) of a PTh solid film formed on an indium−tin oxide electrode was shown in Figure 6. The signal for the reduction (that is, n-type doping) of a PTh solid film was not observed. The oxidation potentials for the porphyrins in dichloromethane solution were indicated by the arrows in Figure 6. The potential is described on the basis of the oxidation potential of ferrocene (Fc) to compare the oxidation profile of the PTh solid with that of the porphyrins, where the oxidation potential of Fc hardly changes by the kind of solvent.[34] The oxidation onset potential of about 0.3 V for PTh in the voltammogram corresponds to the top energy level in the valence band of the PTh solid. The energy level of the highest occupied molecular orbital (HOMO) for the porphyrins is approximated by the oxidation potential. This result is summarized in the energy diagram shown in Figure 7. The energy gap between the HOMO and lowest unoccupied molecular orbital LUMO was estimated from the wavelength of the longest absorption edge of their solid films. Therefore, we can also compare the bottom energy level of conduction band of the PTh solid with the energy level of the LUMO of the porphyrins.

The diagram suggests that electrons can transfer from the ground-state PTh to the excited metal-free porphyrins; namely photoexcited holes in metal-free porphyrins can be injected to the valence band of PTh. Further, the bottom energy level of the conduction band of PTh is more negative than the LUMO energy level of metal-free porphyrins; after all, the photoproduced electrons in PTh can transfer the ground-state metal-free porphyrins. These charge-transfer reactions may cause the photocurrent enhancement and sensitization effects. However, because photoexcited holes in Mgtpp, which has more negative oxidation potential than 0.3 V, cannot be injected to the valence band of PTh, the photocurrent enhancement of the Mgtpp+PTh mixed cell should not occur, resulting in the same level of photocurrent as in the pure Mgtpp cell. Further, the light absorption above 500 nm originated from PTh was hardly used for the photocurrent generation, because the electron transfer from the excited PTh to the ground-state Mgtpp cannot occur. This explains that the action spectrum of the Mgtpp+PTh cell did not follow the absorption spectra above 500 nm corresponding to the absorption by PTh. On the other hand, whether a photoinduced charge transfer can occur between Zntpp and PTh is subtle to judge from the diagram.

The photovoltaic properties of the cells with various metal-free porphyrin+PTh mixed solids under optimum conditions and the oxidation potential of the porphyrins are summarized in Table 3. The ϕ value linearly increased with increasing the oxidation potential of the metal-free porphyrins (see Figure 8) because the hole transfer occurred more easily from the porphyrin to the valence band of PTh due to the increase of the thermodyanic driving force of the hole transfer. From above results, the enhanced photocurrent in the porphyrin/PTh mixture

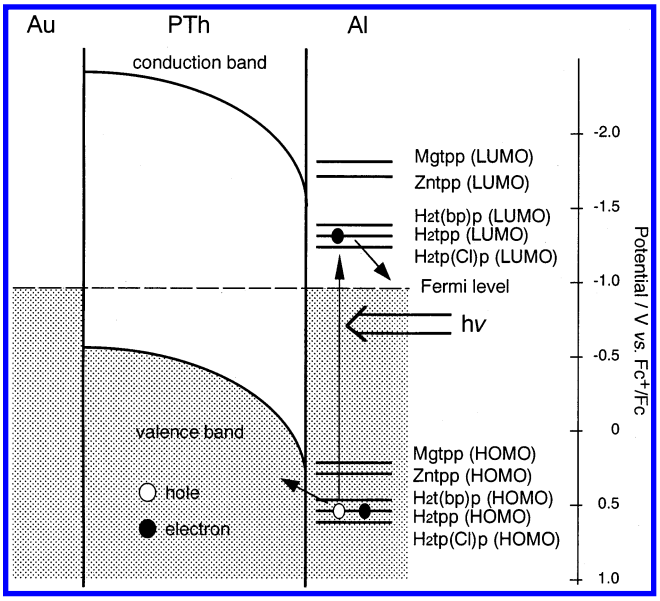

Figure 7. Schematic energy diagram for polythiophene and porphyrins, and schematic concept for hole transfer from photogenerated hole in HOMO of porphyrin to valence band of PTh.

TABLE 3: Performance[a] of Al/Porphyrin+PTh/Au Sandwich-Type Photocells Using Metal-Free Porphyrins with Different Redox Potentials for Al Side Irradiation of Monomeric Light λ under Optimum Condition, and Half-Wave Potentials for Oxidation of Porphyrin $E_{ox}^{1/2}$ [b]

porphyrin	λ (nm)	R	d (nm)	ϕ (%)	V_{oc} (V)	ff	η (%)	$E_{ox}^{1/2}$ (V)
H2t(bp)p	430	0.03	59	4.7	0.57	0.35	0.33	0.45
H2py(bp)3p	430	0.15	38	9.5	0.52	0.33	0.57	0.51
H2tpp	430	0.04	51	11.2	0.59	0.27	0.62	0.53
H2pyp3p	430	0.13	44	13.9	0.62	0.34	1.02	0.58
H2tp(Cl)p	430	0.25	58	18.0	0.60	0.22	0.82	0.63
H2pyp(Cl)3p	430	0.26	45	19.2	0.55	0.32	1.17	0.64

[a] The meaning of symbols is same in Table 1. [b] The oxidation potential was measured in CH_2Cl_2 and was described on the basis of oxidation potential of ferrocene.

TABLE 4: Performance[a] of Al/Porphyrin+PTh/Au Sandwich-Type Photocells Using Porphyrins with Bulky Substituent Groups for Al Side Irradiation of Monomeric Light λ under Optimum Condition and Half-Wave Potentials for Oxidation of Porphyrin $E_{ox}^{1/2}$

porphyrin	λ (nm)	R	d (nm)	ϕ (%)	V_{oc} (V)	ff	η (%)	$E_{ox}^{1/2}$ (V)
H2tpp	430	0.04	51	11.2	0.59	0.27	0.62	0.53
H2tp(2,4,6-Me)p	430	0.02	63	4.32	0.58	0.30	0.26	0.51
H2tp(2,5-OMe)p	430	0.02	60	2.47	0.61	0.32	0.17	0.50
Zntpp	435	0.08	54	10.1	0.47	0.28	0.47	0.29
Zntp(2,5-OMe)p	435	0.05	49	6.1	0.66	0.29	0.41	0.32

[a] The meaning of the symbols is the same in Tables 1 and 3.

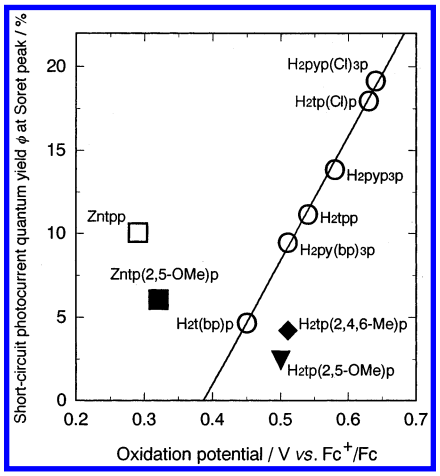

Figure 8. Plots of photocurrent quantum yield ϕ at Soret peak of porphyrins under optimum condition against oxidation potential of porphyrins.

cell can be at least attributed to the effective charge separation by photoinduced hole transfer from porphyrin to PTh.

Effect of Space Distance between Porphyrin and PTh. Zntpp has a more negative oxidation potential than the metal-free porphyrin, and the driving force of hole transfer is eventually smaller, but the ϕ value of the Zntpp+PTh cell was comparable to that of the H_2tpp+PTh cell, as shown in Figure 8. We inferred that the hole transfer easily occurred despite the small driving force because Zntpp molecules can lie very close to the conjugating plane of PTh due to an axial coordination of sulfur atoms in PTh to Zntpp. On the other hand, the conjugating planes of H_2tpp and PTh in the mixed solid can approach by a week $\pi-\pi$ interaction. To examine how the distance between the porphyrin and PTh molecules influences the photocurrent enhancement of the porphyrin+PTh mixed cells, the metal-free and zinc porphyrins with substituent groups in the ortho position in the *meso*-phenyl group of porphyrin, H_2tp(2,4,6-Me)p, H_2-tp(2,5-OMe)p, and Zntp(2,5-OMe)p, were used. The substituted *meso*-phenyl group was assumed to be almost perpendicular to the conjugated porphyrin plane because the rotation of the phenyl group at the single bond was prevented by the substituent group. Therefore the porphyrins cannot lie closely to PTh compared to H_2tpp and Zntpp without the steric hindrance. The mixed cells composed of the nonsubstituted *meso*-phenylporphyrins exhibited larger ϕ values than those composed of the substituted *meso*-phenylporphyrins despite approximately the same thermodynamic driving force for the hole transfer. The photovoltaic properties of the mixed cells and the oxidation potential of the porphyrins are summarized in Table 4.

From these experimental results, it is clearly concluded that the most important factor for determining the photocell performance is whether the photoinduced charge transfer occurs between porphyrin and polythiophene in the mixed solid. When discrete pairs of electron and hole were produced by photoinduced hole transfer from porphyrin to PTh molecules, the Coulomb force between the electron and hole must be much smaller than that between electron and hole in the excited porphyrin or PTh molecule (exciton) because of the larger distance. The photogenerated discrete holes and electrons by such a charge transfer in the vicinity of the Al/organic solid interface were easily separated to opposite directions by the large electric field of more than 10^5 V cm^{-1}. Then the photoproduced holes on PTh molecules hopped through the large PTh molecules and arrived at the remote Au electrode. On the other hand, the photoproduced electrons on porphyrins arrived at the Al electrode in the neighborhood of the porphyrin molecules by a hopping mechanism. Thus, the photocurrent enhancement and sensitization effects by porphyrin dyes were observed for the cell with the H_2tpp+PTh or Zntpp+PTh mixed solid.

Conclusion

In Al/organic solid/Au sandwich-type cells, the photocurrent for irradiation from the Al side was much larger for the mixed cell of porphyrin+PTh than for the pure cell of porphyrin or PTh. The photocharge separation mainly occurred in the narrow region of about 15 nm of organic solid at the Al/organic solid interfaces, where the electric field was as large as 10^5 V cm^{-1}. That is, photons absorbed in the narrow organic solid layer that has potential gradient were effectively used for the photocurrent generation. However, the variation of the short-circuit photocurrent quantum yield depended on the thickness of the film, as shown in Figure 3. This suggests that the photocharge separation occurs also at the PTh/porphyrin interface in the bulk. On the other hand, the observed photocurrent enhancement was not attributed to the magnitude of the electric field at the Al/organic solid interface but to the ease of the photoinduced hole transfer from porphyrin to PTh. That is, when the thermodynamic driving force of the hole transfer was large and the distance between conjugated planes of porphyrin and PTh was short, remarkable photocurrent enhancement was observed.

Acknowledgment. This work was partially supported by Grant-in-Aid for Scientific Research from the Ministry of Education, Science, Sports, and Culture, Japan (Grant 14580536), and by the New Energy and Industrial Technology Development Organization (NEDO) under Ministry of Economy, Trade and Industry (METI).

References and Notes

(1) Halls, J. J. M.; Walsh, C, A.; Greenham, N. C.; Marseglia, E. A.; Friend, R. H.; Maratti, S. C.; Holmes, A. B. *Nature* **1995**, *376*, 498.
(2) Yu, G.; Heeger, A. J. *J. Appl. Phys.* **1995**, *78*, 4510.
(3) Yu, G.; Gao, J.; Hummelen, J. C.; Wudl, F.; Heeger, A. J. *Science* **1995**, *270*, 1789.
(4) Yoshino, K.; Akashi, T.; Morita, S.; Yoshida, M. Hamaguchi, M.; Tada, K.; Fujii, A.; Kawai, T.; Uto, S.; Ozaki, M.; Onoda, M.; Zakhidov, A. A. *Synth. Met.*, **1995**, *70*, 1317.
(5) Roman, L. S.; Andersson, M. R.; Yohannes, T.; Inganas, O. *Adv. Mater.* **1997**, *9*, 1164.
(6) Granstrom, M.; Petritsch, K.; Arias, A. C.; Lux, A.; Andersson, M. R.; Friend, R. H. *Nature* **1998**, *395*, 257.

(7) Angadi, M. A.; Gosztola, D.; Wasielewski, M. R. *J. Appl. Phys*. **1998**, *83*, 6187.
(8) Dittmer, J. J.; Petritsch, K.; Marseglia, E. A.; Friend, R. H.; Rost, H.; Holmes, A. B. *Synth. Met.* **1999**, *102*, 879.
(9) Shaheen, S. E.; Brabec, C. J.; Sariciftci, N. S.; Padinger, F.; Fromherz, T.; Hummelen, J. C. *Appl. Phys. Lett*. **2001**, *78*, 841.
(10) Brabec, C. J.; Shaheen, S. E.; Winder, C.; Sariciftci, N. S.; Denk, P. *Appl. Phys. Lett*. **2002**, *80*, 1288.
(11) Sicot, L.; Fiorini, C.; Lorin, A.; Nunzi, J.-M.; Raimond, P.; Sentein, C. *Synth. Met*. **1999**, *102*, 991.
(12) Sicot, L.; Fiorini, C.; Lorin, A.; Raimond, P.; Sentein, C.; Nunzi, J. *Sol. Energy Mater. Sol. Cells* **2000**, *63*, 49.
(13) Sicot, L.; Geffroy, B.; Lorin, A.; Raimond, P.; Sentein, C.; Nunzi, J. *J. Appl. Phys.* **2001**, *90*, 1047.
(14) Takahashi, K.; Iwanaga, T.; Yamaguchi, T.; Komura, T.; Murata, K. *Synth. Met*. **2001**, *123*, 91.
(15) Takahashi, K.; Nakajima, I.; Yamaguchi, T.; Komura, T.; Murata, K. *Sol. Energy Mater. Sol. Cells*, in press.
(16) Takahashi, K.; Tsuji, K,; Yamaguchi, T.; Komura, T.; Murata, K. *Synth. Met*., in press.
(17) Takahashi, K.; Nanbu, H.; Komura, T.; Murata, K. *Chem. Lett.* **1993**, 613.
(18) Takahashi, K.; Hashimoto, K.; Komura, T.; Murata, K. *Chem. Lett.* **1994**, 269.
(19) Takahashi, K.; Nakamura, J.; Yamaguchi, T.; Komura, T.; Ito, S.; Murata, K. *J. Phys. Chem. B* **1997**, *101*, 991.
(20) Takahashi, K.; Higashi, M.; Tsuda, Y.; Yamaguchi, T.; Komura, T.; Ito, S.; Murata, K. *Thin Solid Films* **1998**, *333*, 256.
(21) Takahashi, K.; Goda, T.; Yamaguchi, T.; Komura, T.; Murata, K. *J. Phys. Chem. B* **1999**, *103*, 4868.
(22) Alder, A. D.; Longo, R. F.; Finarelli, J. D.; Assour, J.; Korsakoff, L. *J. Org. Chem*. **1967**, *32*, 476.
(23) Alder, A. D.; Longo, R. F.; Kampas, F.; Kim, L. *J. Inorg. Nucl. Chem*. **1970**, *32*, 2443.
(24) Murata, K.; Ito, S.; Takahashi, K.; Hoffman, B. M. *Appl. Phys. Lett*. **1997**, *71*, 674.
(25) Takahashi, K.; Terada, T.; Yamaguchi, T.; Komura, T.; Murata, K. *J. Electrochem. Soc*. **1999**, *146*, 1717.
(26) Twarowski, A. J.; J. Albrecht, A. C. *J. Chem. Phys*. **1979**, *70*, 2255.
(27) Shing Y. H.; Loutfy, R. O. *J. Appl. Phys*. **1981**, *52*, 6961.
(28) Kampas, F. J.; Yamashita, K.; Fajar, J. *Nature* **1980**, *284*, 40.
(29) Harima, Y.; Takeda, K.; Yamashita, K. *J. Phys. Chem. Solids* **1995**, *56*, 1223.
(30) Kaneto, K.; Hatae, K.; Nagamatsu, S.; Takashima, W.; Pandey, S. S.; Endo, K.; Rikukawa, M. *Jpn. J. Appl. Phys.* **1999**, *38*, L1188.
(31) Kunugi, Y.; Harima, Y.; Yamashita, K.; Ohta, N.; Ito, S. *Chem. Lett*. **2000**, 260.
(32) Harima, Y.; Furusho, S.; Okazaki, K.; Kunugi, Y.; Yamashita, K. *Thin Solid Films* **1997**, *300*, 213.
(33) Harima, Y.; Furusho, S.; Kunugi, Y.; Yamashita, K. *Chem. Phys. Lett*. **1996**, *258*, 213.
(34) Gritzner, G.; Kuta, J. *Pure Appl. Chem*. **1984**, *56*, 461.